Available online at www.sciencedirect.com
SCIENCE DIRECT
Earth and Planetary Science Letters 245 (2006) 373–388
EPSL
www.elsevier.com/locate/epsl

The Hinlopen Slide: A giant, submarine slope failure on the northern Svalbard margin, Arctic Ocean

Maarten Vanneste *, Jürgen Mienert, Stefan Bünz

Department of Geology, University of Tromsø, Dramsveien 201, N-9037 Tromsø, Norway

Received 12 December 2005; received in revised form 24 February 2006; accepted 27 February 2006
Available online 5 April 2006
Editor: M.L. Delaney

Abstract

New swath bathymetry data unveil a giant, submarine landslide located at the mouth of the Hinlopen transverse trough on the northern Svalbard margin, Arctic Ocean. Despite the relatively small drainage and slide scar areas, the Hinlopen Slide is exceptional in volume, headwall height and dimensions of the rafted blocks. From the c. 2200 km^2 large headwall area, approximately 1350 km^3 of Plio-Pleistocene sediments have been evacuated from the continental margin to the Nansen Basin. The escarpment heights are unprecedented, exceeding 1400 m, whereas the rafted blocks observed in the intermediate part of the slide area are up to 450 m high and more than 5 km wide. These characteristics make the Hinlopen Slide one of the largest landslides worldwide, and the first mapped mega-slide in the Arctic Ocean. Within the amphitheatre-shaped slide scar area, a composite set of escarpments and multiple, roughly planar slip surfaces occur, as well as detached sediment ridges adjacent to the outer escarpment, arcuate pressure ridges in debris lobes and isolated slump debris or blocks. From this complex slide scar geomorphology, we infer that the Hinlopen Slide was a translational, multi-phase slope failure that developed retrogressively. The slide has not been dated yet; however, the geophysical data suggest a relatively young age, though probably pre-Holocene, inferred from the pattern of sediment infill within the slide scar area derived from the Hinlopen cross-shelf trough. A submarine landslide with these dimensions could have created a devastating tsunami, although its potential depends on sea ice conditions as well as the time lags of the multi-phase, retrogressive movement. Climate changes and the response of ice sheets, ocean-current systems, sediment delivery and seismicity related to glacio-isostatic deformation appear as critical factors controlling stability on glaciated margins.

Keywords: high-latitude submarine slope failure; Arctic Ocean; Northern Svalbard margin; headwall; rafted blocks; Hinlopen; glaciated margin; swath bathymetry

1. Introduction

Recent improvements in seabed (e.g. swath bathymetry) and sub-surface mapping techniques (high-resolution 3D seismic imaging) have revealed a wealth of slide scars and a diversity of related deposits on many of the world's continental margins [1]. Despite their abundance worldwide, submarine landslides are virtually unknown in the Arctic Ocean, mainly due to severe ice conditions that have previously hindered detailed investigations. Sediment failure is nevertheless common on glacial margins and covers a wide spectrum of dimensions, ranging from relatively small-scale mass wasting processes in fjords to massive slides affecting several tens

* Corresponding author. Tel.: +47 77646505; fax: +47 77645600.
E-mail address: maarten.vanneste@ig.uit.no (M. Vanneste).

0012-821X/$ - see front matter © 2006 Elsevier B.V. All rights reserved.
doi:10.1016/j.epsl.2006.02.045

of thousands of km^2 [2]. High-resolution geophysical data from the passive Norwegian margin reveal several large seabed failures that have happened during the Holocene, e.g. the Storegga [3], the Trænadjupet [4] and the Andøya Slides [5] (Fig. 1), whereas the Quaternary records also show evidence of buried, large-scale failures [6]. These slope failures have several aspects in common: their headwalls lie close to the shelf break; they occur adjacent to or within major sediment depocentres fed by ice streams [7]; they happened primarily during interglacial periods [6]; their dimensions are orders of magnitude larger than submarine slope failures on active margins or in lower-latitude settings; and they often show close links to intra-plate seismo-tectonic activity related to glacio-isostatic rebound following the retreat of the Fennoscandian ice sheet [8,9]. The influence of climate on slope stability is also evident in sedimentation variability due to both changing oceanographic patterns and ice sheet dynamics [10]. With global warming looming [11] and the potential of submarine landslides to create tsunamis [12,13], climatic forcing on slope stability – particularly on glacial margins – represents a threat to communities and environments on the coastal lowlands. Therefore, understanding submarine slope failure and its consequences in Polar Regions is of vital importance, especially since ice dome melting and subsequent isostatic rebound are currently taking place in Antarctica [14,15] and Greenland [16,17].

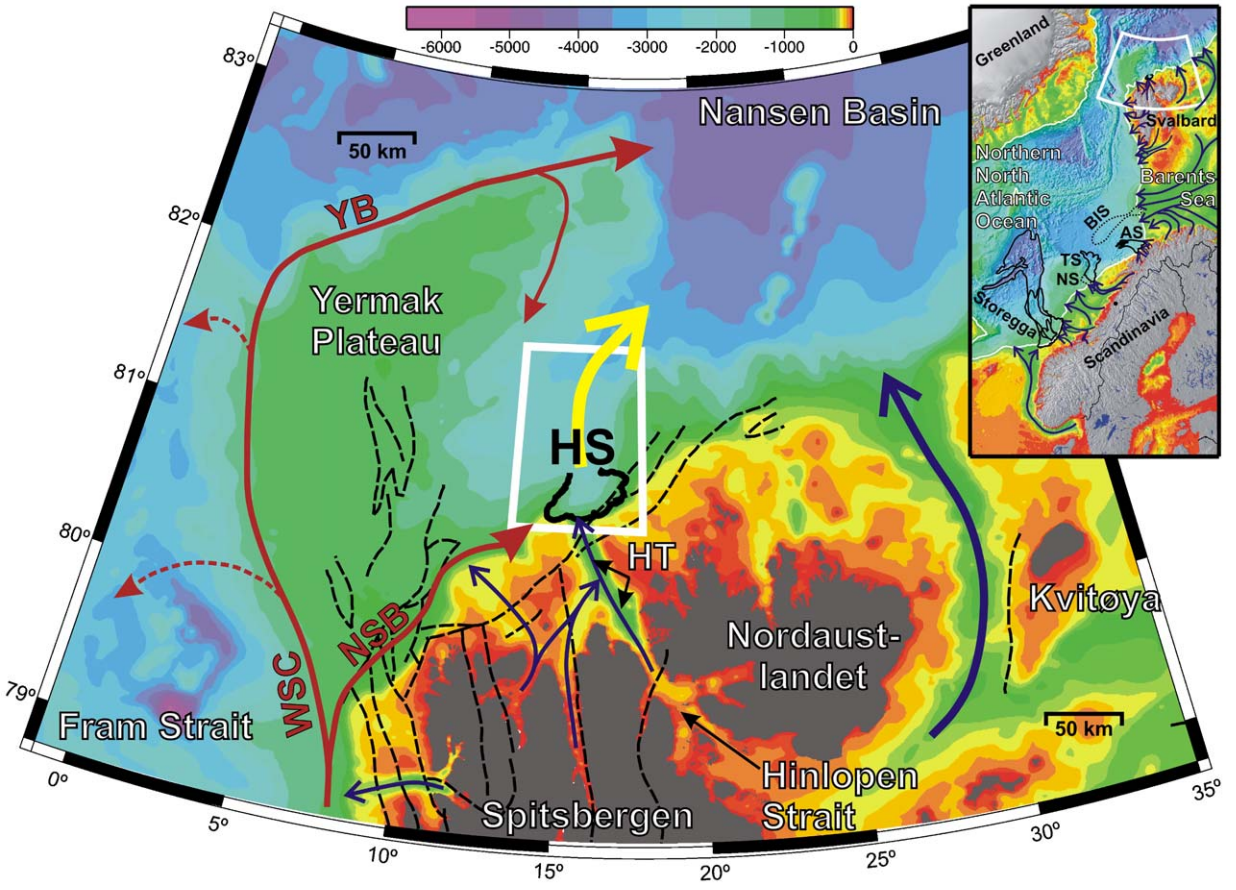

Fig. 1. Structural map of the northern Svalbard margin, bordered by the Yermak Plateau and opening towards the Nansen Basin, Arctic Ocean (for location, see inset). The headwall of the Hinlopen Slide (HS) lies at the mouth of the prominent Hinlopen cross-shelf trough (HT). The yellow arrow shows the evacuation direction of the slide material. Black stippled lines represent major fault systems, of which two faults intersect with the eastern headwall area. Note the widening of the shelf and upper slope area off Nordaustandet compared to Spitsbergen. Blue arrows indicate ice streams draining the Eurasian ice sheet during peak glacial times across the shelves [7,20]. Presently, the area is influenced by the inflow of temperate warm water branches (dark-red arrows), the North-Svalbard Branch (NSB) and the Yermak Branch (YB), tapped off from the West-Spitsbergen Current (WSC). The study area (white box) is highlighted in Fig. 2. The inset also shows the outlines of other major submarine landslides (solid: Holocene, dashed: pre-Holocene) and the approximate ice margin during the Weichselian glaciations (white line). Abbreviations used: AS = Andøya Slide; BIS = Bear Island Slide; HS = Hinlopen Slide; NS = Nyk Slide; TS = Trænadjupet Slide.

The objectives of this paper are to present a new geophysical data set, consisting of swath bathymetry and single-channel seismic reflection data, and to discuss the slide scar geomorphology, estimates of released volume, and the implications of a giant submarine slope failure at the border of the Arctic Ocean. Since the slide headwall lies in front of the Hinlopen Trough, we have named this submarine slope failure the *Hinlopen Slide*.

2. Geological setting

The architecture of high-latitude continental margins displays the interaction between tectonic, glacial and oceanographic processes. The northern Svalbard margin (Fig. 1) belongs to the passive Eurasian margin of the Arctic Ocean, and has probably a longer history of subsidence and deposition compared to the sheared western margin, due to earlier continental separation [18]. The Eurasia Basin opened c. 60–55 Ma with the separation of the continental Lomonosov Ridge from the northern Svalbard and Barents shelf margin, and subsequent – and since then continuous – seafloor spreading along the ultra-slow Gakkel Ridge [19]. Some fault zones sub-parallel to the coast might be related to this rifting process [18]. The prominent Yermak Plateau, confined by the 800 m isobath, marks the western border of the northern Svalbard margin. To the east, the margin opens towards the deep Nansen Basin. The continental shelves offshore Spitsbergen and Nordaustlandet are fairly flat and 50 to 100 km wide, whereas the upper slope area widens off Nordaustlandet (Fig. 1).

The presence and dynamics of glaciers and ice streams during Plio-Pleistocene glaciations have had a pronounced effect on both sedimentation and erosion on high-latitude continental margins, including the northern Svalbard margin [20]. An increase in ice-rafted debris in deep boreholes dated at 2.6–2.3 Ma indicates that glaciers advanced to open seas around that time [21]. Numerical ice-sheet modelling suggests that the vast Weichselian ice sheets extended to the shelf edges [22,23], although no ground-truthing is available from the northern Svalbard margin. The presence of ice sheets has consolidated and eroded the sediments on the shelf banks, whereas fast-flowing ice streams scoured cross-shelf troughs and pushed large volumes of terrigenous sediments beyond the shelf break during glacial times, resulting in shelf progradation and stacked glacigenic debris flow deposition on the upper slope [7,20]. This was for example the case for the Hinlopen Trough as well as the glacial trough between the islands of Kvitøya and Nordaustlandet (Fig. 1) [24], although more extensive fan systems implying larger drainage developed in front of cross-shelf troughs further east (e.g. Franz Victoria Trough) and on the (south-)western Svalbard margin [25]. Sediment transport through the Hinlopen strait and trough endured during interglacial times [26]. The total sediment thickness on the northern Svalbard margin ranges from several hundreds of metres to c. 9 km, of which the upper Plio-Quaternary cover mainly consists of stacked glacigenic debris flow and glacimarine deposits [24]. Sediments are furthermore partly reworked by contour currents, related to the inflow of the North-Svalbard and Yermak Branches, which are both derived from the temperate West-Spitsbergen Current [27,28]. The North-Svalbard Branch flows along the shelf and upper slope (between c. 100–200 and 600–800 m depth) and supplies the main portion of Atlantic Water to the Arctic Ocean [27,28].

2.1. Data and methods

In this paper, we present newly collected swath bathymetry data combined with single-channel seismic reflection data, all collected onboard R/V Jan Mayen (University of Tromsø) during October 2004.

The swath bathymetry data were acquired with a motion-compensated Kongsberg Simrad EM300 system, mounted in the hull of the vessel. The system operates at a nominal sonar frequency of 30 kHz, and results in an angular coverage of 150 degrees using 135 beams. Sound velocity through the water column was integrated from CTD stations acquired prior to and during the bathymetry surveying. Data processing consisted of quality control, cleaning and smoothing of the navigation data, noise reduction, and removal of the outer beams using the software package Neptune. Final gridding, imaging and calculation of slope angle were done in GMT [29], with cell size of 75 m by 75 m. The swath bathymetry data cover an total area of c. 4795 km^2 between 80.60 °N–81.65 °N latitude and 13.0 °N–17.5 °N longitude, with water depths ranging from a mere 100 to 2800 m (Fig. 2).

We collected single-channel seismic reflection profiles along key transects across the Hinlopen headwall area, guided by the swath bathymetry. The airgun array consists of a double sleeve gun towed at short distance behind the ship at 4 m submersion depth. The guns were fired at 120–130 bars with a small time delay in order to obtain a sharper source signal. As a receiver, we used a high-resolution single-channel streamer, floating at near-zero offsets behind the source. The data were digitally recorded using Elics-Delph2 at 2 kHz sampling rate. The shooting was set on 8 s time interval, resulting in an average shot spacing of c. 22 m. Both acoustic penetration and signal-to-noise ratio change significantly,

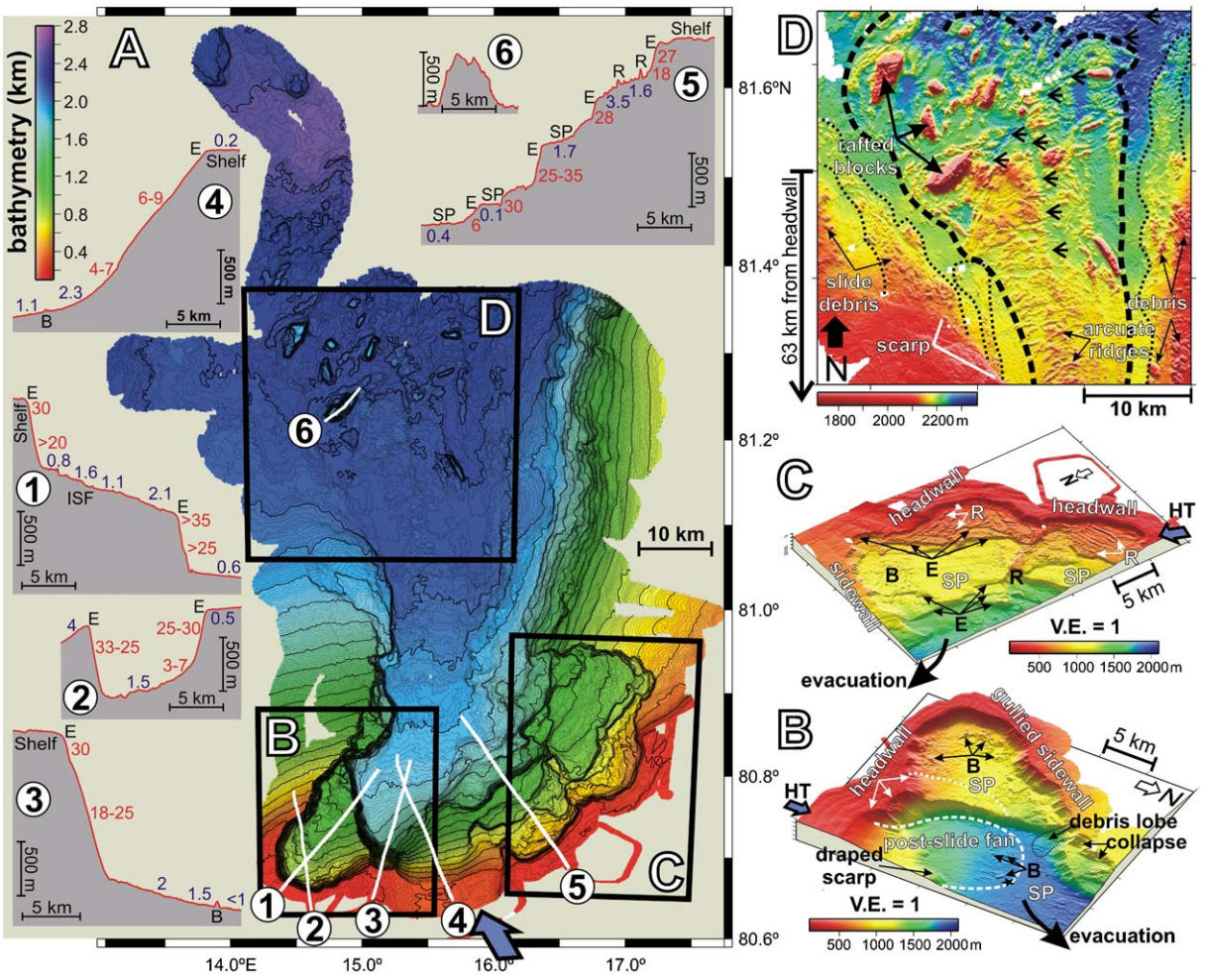

Fig. 2. (A) Swath bathymetry image (c. 4795 km^2) of the Hinlopen Slide scar area on the northern Svalbard margin off the mouth of the Hinlopen Trough (HT). Contour interval is 10 m (thin) respectively 100 m (bold). The tracks, highlighted in the insets, nicely illustrate the different characteristics of the escarpments discussed in the text (e.g. slope and throw). Numbers along the tracks represent slope angles in degrees (red: maximum angles of escarpment, blue: mean dip of slip surface). The seismic profile corresponding to track 4 is shown in Fig. 4A. The blue arrow south of the headscarp represents the sediment inflow from the Hinlopen Trough. The boxes mark the locations of the illuminated pseudo-3D views shown at the right (B–D). The western (B) respectively eastern (C) slide scar areas are displayed with a vertical exaggeration 1:1. The white dashed line (B) marks the outer limit of the post-slide sediment lobe derived from the Hinlopen Trough whereas the star represents the location of the sediment core containing ice-rafted debris discussed in the text. The black dashed curves (D) delineate blocky slide debris lobes, comprising both arcuate ridges and gigantic rafted blocks. Some glide tracks are indicated by black arrows (D). (Annotations: B = block, E = escarpment, ISF = irregular sea floor, R = detached sediment ridge, SP = slip plane).

due to the high spatial variability of the sub-surface in the study area. The standard data processing sequence included bandpass frequency filtering, muting and automatic gain control.

3. Results: characteristics and dimensions of the Hinlopen Slide

3.1. Characteristics of the Hinlopen Slide

Evidence of large-scale slope failure in front of the Hinlopen cross-shelf trough bordering the Arctic Ocean has first been reported in 1999 based on single-beam echo-sounder and side-scan sonar investigations [30]. However, our new swath bathymetry data demonstrate in much greater detail the geomorphologic variability of the slide scar area (Fig. 2), improving our understanding of slope failure and providing better control on volumetric calculations. Despite its smaller spatial extent, the headwall area of the Hinlopen Slide is somehow similar to the Storegga Slide scar area on the mid-Norwegian margin [3,31]. The well-developed headwall of the Hinlopen Slide is c. 120 km long and forms an amphitheatre-like structure. The slide scar has

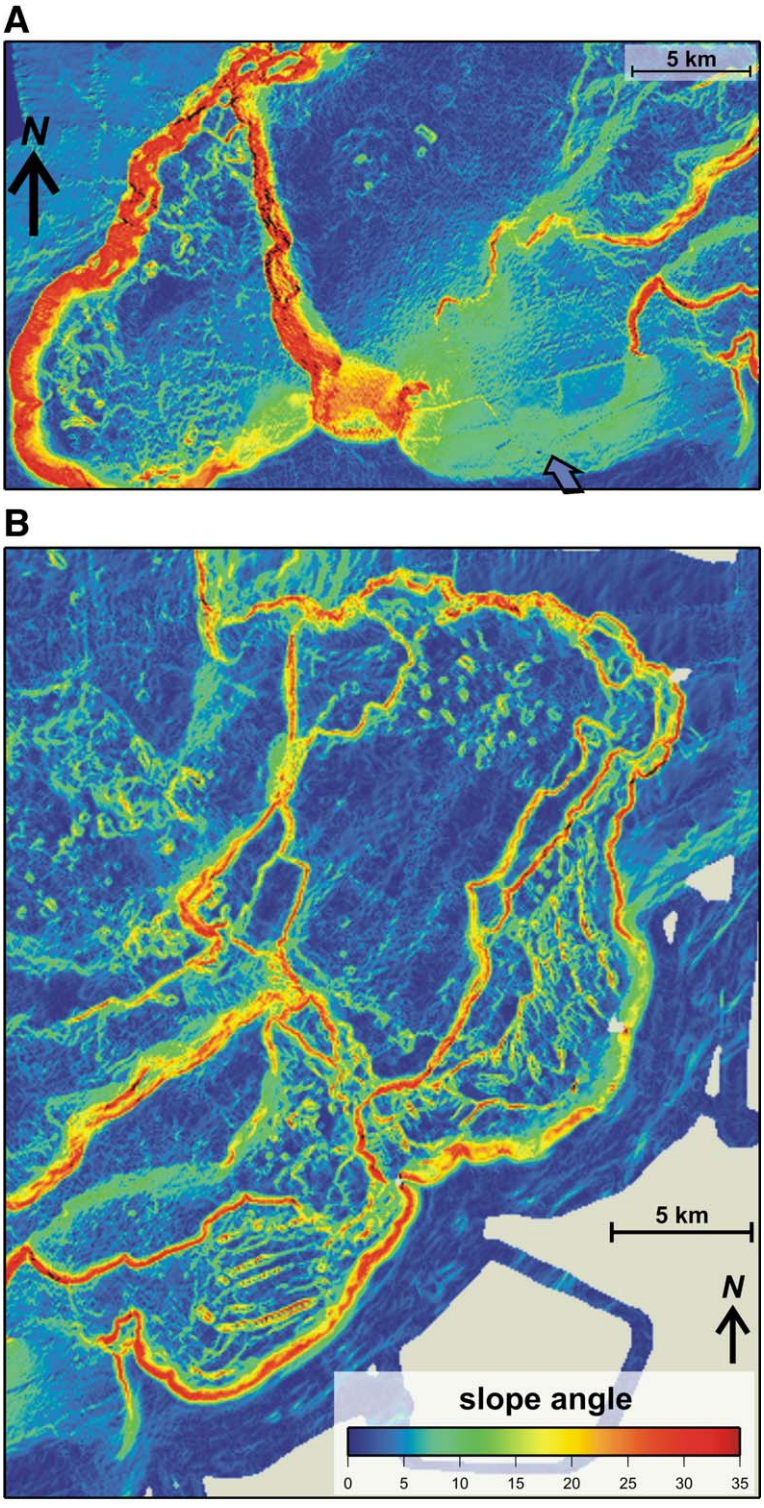

Fig. 3. (A) Seabed slope map for the western part of the slide scar area, corresponding to the pseudo-3D view shown in Fig. 2B. The blue arrow at the southern headscarp represents the sediment in fill derived from the Hinlopen Trough. (B) Seabed slope map for the eastern part of the slide scar area, corresponding to the pseudo-3D view shown in Fig. 2C. The outer and inner escarpments are very steep, dipping up to 35°, with exception made for the headscarp in front of the Hinlopen Trough where the dip angle is significantly lower (< 10°) partly due to post-slide sediment infill. The slip surfaces dip gently (<3°), and are hummockier in the eastern part compared to the western part of the headwall area. The colour codes are identical for both maps.

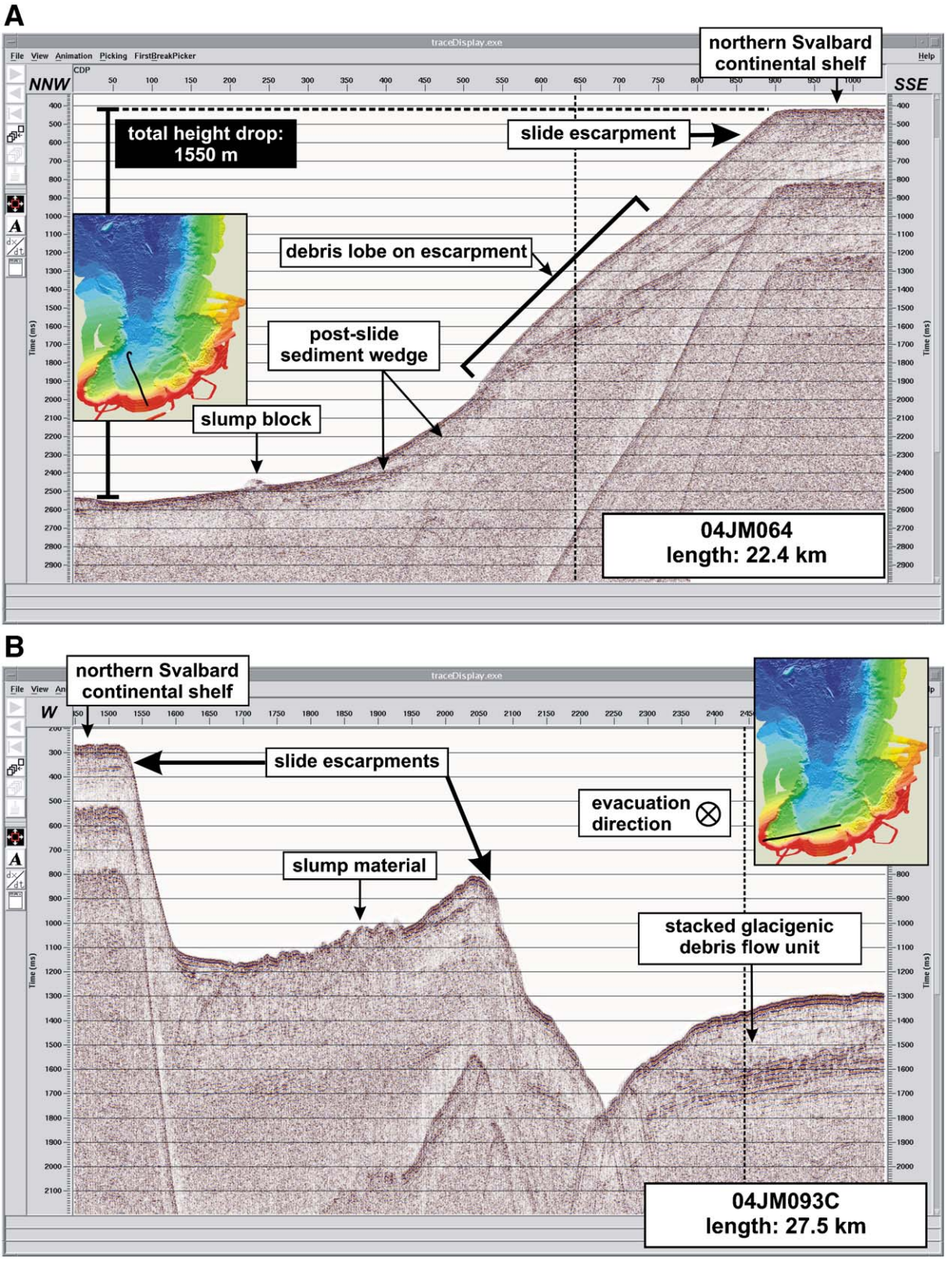
A
traceDisplay.exe
File View Animation Picking FirstBreakPicker
Help
NNW
SSE
CDP
Time (ms)
northern Svalbard continental shelf
total height drop: 1550 m
slide escarpment
debris lobe on escarpment
post-slide sediment wedge
slump block
04JM064
length: 22.4 km
B
traceDisplay.exe
W
northern Svalbard continental shelf
slide escarpments
evacuation direction
slump material
stacked glacigenic debris flow unit
Time (ms)
04JM093C
length: 27.5 km

a maximum width of 58 km and narrows downslope to less than 20 km, forming a pronounced bottle-neck. The headwalls lie close to the shelf break, in water depths between 200 and 500 m. The slide scar area reveals a multitude of impressive escarpments delineating distinct planar failure surfaces. From the bathymetry (Fig. 2), we recognise three distinct morphological provinces in the slide area: the western part of the headwall area (Fig. 2B, Fig. 3A); the eastern part of the headwall area (Fig. 2C, Fig. 3B); and the intermediate part downslope the bottle-neck (Fig. 2D).

In the western part of the headwall area (Fig. 2B), the gullied outer scarp forms a prominent > 600 m deep and 12.5 km wide depression, draped with some slide blocks and debris (Fig. 3A). A second major escarpment cuts away another 500–600 m of sediments some 14 km further downslope. As a result, the total height drop exceeds 1600 m from the undisturbed shelf area to the deepest slip surface adjacent to the lowermost escarpment (Fig. 2, transect 1). The maximum headwall height measures an unprecedented 1400 m where these two major escarpments merge (Fig. 2, transect 3). Few isolated slide blocks are present on the deepest slip surface (Fig. 3A). The limited slide debris and small number of slump blocks observed indicate that the western part of the slide scar area was properly evacuated. The slip surfaces dip gently (<3°), whereas the slide escarpments have steep slopes up to 35°. The headscarp in front of the Hinlopen Trough is an exception with slope angles less than <10° (Fig. 3A). Both the swath bathymetry data (Fig. 2B, Fig. 3A) and seismic reflection data (Fig. 4) reveal post-slide sediment infill restricted to the southern part of the slide scar area. First, we observe a sediment wedge on top of the slip surface immediately downslope the headwall (Fig. 4A). This sediment fan is about 150 m thick (roughly 200 ms two-way travel time), and fades out approximately 12 km into the slide area. Second, there is a positive relief feature, interpreted as a debris lobe, deposited onto the headscarp (Fig. 4A). Third, a seismic profile across this positive relief structure indicates its semi-transparent signature (Fig. 4B), which is typical for stacked glacigenic debris flow units deposited as a result of ice stream dynamics [32]. These observations suggest that the sediments are glacigenic in origin and are mainly derived from the Hinlopen Trough, draping the escarpment and thereby contributing to a gentler dip (e.g. Fig. 2, transect 4, Fig. 3). Taking this sediment infill into account, then the maximum escarpment height exceeds 1500 m.

The eastern part of the headwall area is strikingly different and more complex (Fig. 2C, Fig. 3B). We identify a composite set of smaller detachment surfaces with low dips (<3°) separated by steep escarpments (up to 35°) between 180 and 400 m high (Fig. 2, transect 5). One prominent ridge structure extends into the slide scar perpendicular to the headwall. This ridge rises 200 m above the seabed and delineates different instability zones and phases that somehow spared this ridge from failing. Immediately downslope from and sub-parallel to the upper headwall segments, several extensional and partly eroded sediment ridges occur (Fig. 2, transect 5). Their length varies between several hundreds of metres to over 4 km. The spacing and height of these extensional ridges decrease downslope, similar to observations from the Trænadjupet [4] and Storegga slides [33]. These detached ridges probably originate from consecutive stretching, faulting and back-tilting following sediment removal at the toe and indicate the presence of a weak basal layer underneath stiff sediments [4,33]. The hummocky seabed morphology characterised by debris, detached ridges and slump blocks (Fig. 3B), indicates that the eastern scar area has not been fully evacuated, probably pointing towards less vigorous mass movement. There is no evidence of post-slide sediment infill in this part of the slide area.

The intermediate part of the slide area, from c. 63 km from the headwall and downslope from the bottle-neck (Fig. 2D), displays several accumulated debris lobes. Some contain small-scale seabed irregularities and slump deposits, and are located close to the margins of the slide area. The main debris accumulation occupies the central part, and consists of transverse positive relief features. These arcuate and irregular ridges are tens of metres high, and typically originate from compressional deformation during movement. In the distal part beyond these pressure ridges, enormous rafted blocks appear. The largest of these rafted block rises 452 m above the

Fig. 4. (A) This down-slope seismic profile 04JM064 across the Hinlopen headwall shows evidence of post-slide sediment infill into the slide scar area. First, a sediment fan or wedge extends several km into the slide area from the foot of the headwall. Second, a positive relief structure interpreted as a glacigenic debris lobe covers the lower part of the main escarpment. The sediment fan and debris lobe are thought to originate from post-slide glacigenic sediment infill from ice stream draining through the Hinlopen Trough during peak glacial times. The profile corresponds to transect 4 on Fig. 2. (B) This seismic profile 04JM093C across the western slide complex characterised by the double major escarpments provides evidence for glacigenic post-slide sediment infill. This profile crosses the post-slide debris lobe on the main Hinlopen Slide escarpments revealing the chaotic and transparent signature with irregular surface typical for stacked glacigenic debris flows, thereby providing indirect evidence of the pre-Holocene timing of the Hinlopen Slide. The maps show the locations of the seismic profiles. The vertical dashed lines mark the intersection of the two seismic lines.

surrounding seabed and has an elongated footprint covering an area of 8.7 km^2 (maximum 5.4 by 2.1 km) (Fig. 2, transect 6). This block contains a total of 1.89 km^3 of sediments. The observed smooth stripes throughout the debris lobe might represent glide tracks along which individual rafted blocks have moved due to gravity [34]. The accumulated debris observed on our data set obviously does not compensate for the total volume of sediments removed from the headwall area (see below), indicating that the bulk of the sediment volume released by the slope collapse has been evacuated to the deep Nansen Basin.

3.2. Volume estimation and run-out

In order to estimate the total mobilized volume, we have reconstructed the pre-slide bathymetry within the well-defined slide scar by removing the bathymetry data within the scar and subsequently interpolating (triangulation) the remaining undisturbed bathymetry. Subtracting these grids yields a total volume of c. 1350 km^3 of sediments evacuated from a relatively small headwall area of c. 2200 km^2. This gives an *average* thickness of c. 610 m for the removed sediment slab. For comparison, the *maximum* thickness for the Storegga Slide is c. 400 m [35].

The total area affected by the slope failure and the maximum run-out distance are more difficult to assess due to the sea ice cover in the distal part of the northern Svalbard margin. Additionally, the post-failure stage or mobility of a submarine landslide typically involves material transformation from solid to liquefied state with the detachment of slabs that subsequently disintegrate in debris avalanches, debris flows and ultimately turbidity currents [2,36]. As discussed above, our data reveal the presence of some debris lobes comprising the massive rafted blocks that have accumulated at about 60 km from the headwall (Fig. 2D). The swath bathymetry data presented here, however, do not cover the entire slide-affected area. The existence of debris flow deposits that have evolved from the Hinlopen Slide in the Nansen Basin in water depths approaching 4 km for example implies run-out distances of at least 300 km, a process probably facilitated by hydroplaning [37]. We also have to bear in mind that the most mobile and therefore distal slide-related deposits are likely to be turbidites, which could have travelled even further into the Arctic Ocean, and as such, the slide affected area can be very large [37]. The mobility of the slide material is probably related to the height of the headwalls. The enormous escarpment height of several hundreds of metres to more than 1400 m provides a substantial potential energy, which is transformed into kinetic energy upon failure and could add to the slide mobility. How and when the mobilised sediments are remoulded to a more liquefied state and subsequently transported as debris flows remain unknown. Since little slide material remains within the headwall area (Fig. 2) in combination with long run-out distances, one might furthermore expect transformation from slabs to flows already in the failure area, even though several trunks of consolidated sediment (rafted blocks) were not remoulded during the downslope flow.

4. Discussion

4.1. Failure mechanism

Submarine mass movements can be classified according to the geomorphology and characteristics of the failure surface [38]. The well-defined arcuate headwall, the extended sidewall, and the multiple and roughly planar sliding surfaces separated by steep linear escarpments with large throws characterise the Hinlopen Slide as a translational, multi-phase and retrogressive submarine slope failure. The ratio of total height drop to run-out distance of the Hinlopen failure gives a Skempton ratio of c. 0.01, categorising it as a translational slide (<0.15) for which rafted blocks constitute a well known feature [2,38]. The retrogressive nature is also supported by the huge amount of sediments evacuated through the relatively narrow bottle-neck, and the presence of detached sediment ridges adjacent to the headwall segments in the eastern part of the slide scar area. The central part of the headwall area appears to have been dislodged first, creating the steep escarpments as well as the bottle-neck. It is the removal of support at the toe that subsequently led to failure of the adjacent slopes in several phases. The location of the headscarp at the shelf edge indicates a halt of retrogressive failure due to either overconsolidated, stiff shelf sediments or changes in dip angle, or both. The difference in morphology and evacuation between the western and eastern slide scar areas may furthermore reflect spatially varying sedimentation patterns through time. This could be related to the inflowing ocean currents from the west following regional contours along the upper slope.

The conditions leading to failure are difficult to elucidate and often form a complex pattern of interacting processes [2]. The most obvious pre-conditional factors promoting failure on the northern Svalbard margin are high sedimentation rates combined with spatial and temporal variability in sedimentation, glacio-tectonic processes and glacio-isostatic movement.

The northern North-Atlantic margins are characterised by strong climate-controlled changes in sedimentation [4,39–41]. Sedimentation rates in the study area are suspected to be periodically high, considering its location in front of a major cross-shelf trough through which significant amounts of glacial erosional products are pushed by fast-flowing ice streams that are subsequently delivered to the shelf break, even though the Hinlopen Trough was probably not the main ice stream pathway for drainage of the Eurasian ice sheets during the Late Quaternary [20,39]. Correlation with deep seismic data crossing the western part of the slide scar indicates that the deepest slip surface corresponds roughly with sediments deposited at the beginning of northern hemispheric cooling which was initiated around 2.6–2.3 Ma [24]. This could hint towards climate control on slope stability, and explain the unique height of the escarpment. Additionally, translational sediment displacement is common in mechanically inhomogeneous sediment successions; in other words, in sequences containing bedding layers with different geotechnical and lithological properties [4,42]. Such variation in depositional history is evidenced by high-resolution seismic reflection profiles across the shoulders of the slide area (Fig. 5). The seismic profiles reveal the presence of semi-transparent glacigenic debris flow units as well as wavy contourites probably deposited under marine or glacio-marine conditions, which indicate the sedimentation response to glacial–interglacial cycles (Fig. 5). Branches of Atlantic Water masses ultimately derived from the Norwegian Atlantic Current flow into the study area as the North-Svalbard Branch (Fig. 1). From studies on the Norwegian margin we know that the Norwegian Atlantic Current system has deposited contourite drifts over a large lateral extent [10]. Therefore, we infer that the deposition of geotechnically-weaker contourites brought in by the North-Svalbard Branch may explain the occurrence of several failure planes over a fairly large area (up to several tens of square kilometres) north of Svalbard as well. This would especially be the case where the morphology of the upper slope along which the currents flow changes, i.e. in the immediate vicinity of the Hinlopen headwall area (Fig. 1). In fact, the setting of the Hinlopen Slide is similar to Storegga's, in the sense that these passive margin segments have both been fed by large amounts of glacial sediments from ice streams alternated by contour-current deposits. Therefore, we consider the Storegga Slide analogue as a plausible scenario to explain this giant slide in the Arctic Ocean. In this scenario, a gravitational unstable situation arises from the overloading of contouritic (marine) clays which are prone to the development of excess pore pressure when massive glacigenic debris flows are rapidly deposited on top (strain softening behaviour) [3,36,43]. The occurrence of multiple slip surfaces fits this model, considering the link between sedimentation and climate variability.

Seismicity related to glacio-isostatic processes is the prime candidate as a potential trigger for slope failure north of Svalbard. Earthquake swarms may progressively prepare the sediments for failure through creeping, cracking or block detachment until displacement occurs [2]. Since the adjacent shelf areas have probably been covered by a thick ice mass [22,23], crustal deformation may have generated seismo-tectonic activity in the area, with magnitudes significantly larger than expected from passive margin segments, as evidenced for Scandinavia [8]. We also note that the eastern part of the slide scar complex overlies some major faults which could have contributed to failure (Fig. 1). Neo-tectonic maps of Svalbard furthermore illustrate recent seismicity both on Nordaustlandet and in the immediate vicinity of the headscarp [44], so earthquakes could have played a decisive role in triggering the landslide when crustal deformation and glacio-tectonic activity had higher intensity. Good examples can also be found from the seismo-tectonically quiescent eastern Canadian margin that experienced extensive Pleistocene glaciations, and where major earthquakes probably related to glacio-isostatic tectonic adjustment (e.g. Grand Banks M7.2 event in 1929) and subsequent slope failure have happened [45,46].

4.2. Timing of failure?

The age of the giant Hinlopen landslide is not yet known. Dating of core samples is presently being undertaken, but becomes complicated due to low concentrations of planktonic foraminifera in the samples. Based on the geophysical data, the slide is probably a relatively recent feature, but not later than the time when the Svalbard ice sheet started disintegrating. The slip surfaces look rather fresh; neither the seismic data nor the swath bathymetry data show evidence for significant post-slide sediment infill, except for the sediment fan deposited at the mouth of the Hinlopen Trough. Gravity cores retrieved little to no normally-consolidated sediments overlying the slip planes. Additionally, core-log analyses indicated high bulk densities (>2.0 g/cm^3) at the bottom, suggesting compacted sediments that may represent the top of the slip surfaces. One core from the distal part of the sediment lobe, however, recovered a continuous sediment record revealing a high ice-rafted debris content that gradually decreases upwards with little clasts in the uppermost part. This may represent the sedimentation change between glacial to Holocene conditions.

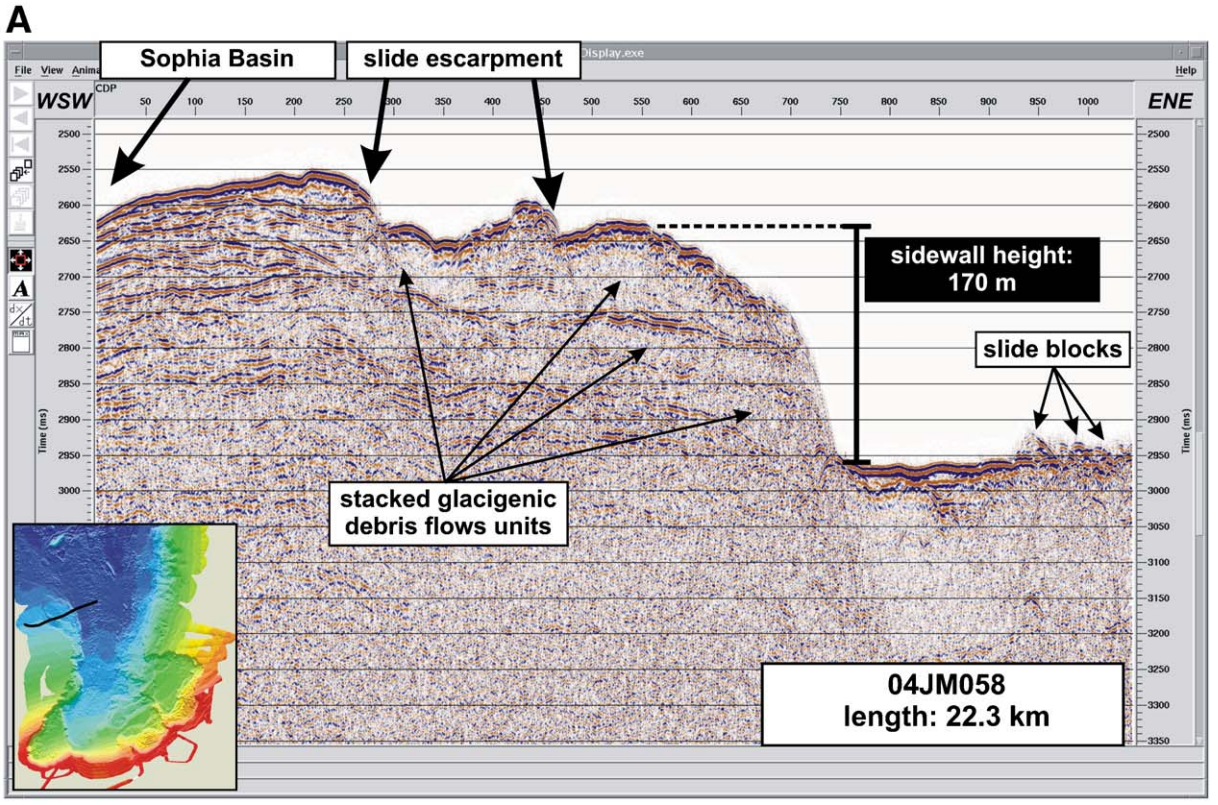
A
Sophia Basin
slide escarpment
WSW
ENE
CDP
sidewall height:
170 m
slide blocks
stacked glacigenic
debris flows units
04JM058
length: 22.3 km
Time (ms)

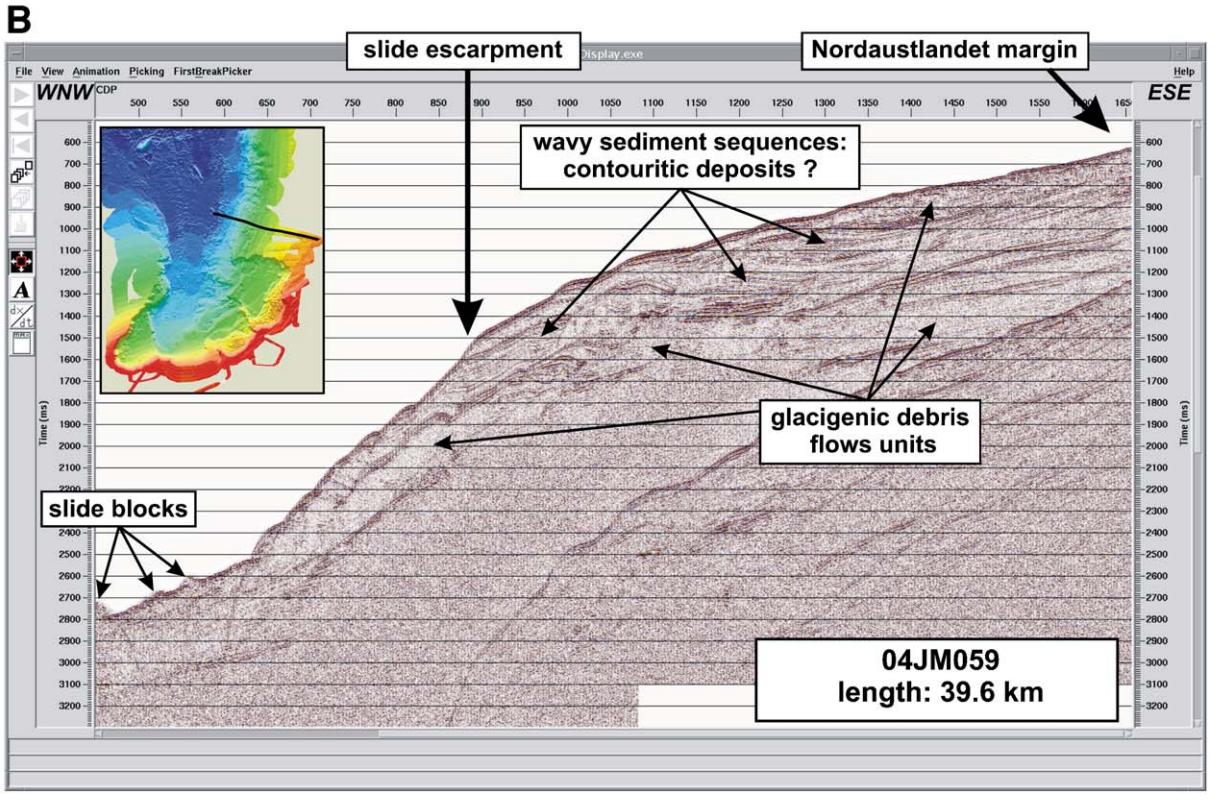
B
slide escarpment
Nordaustlandet margin
WNW
ESE
CDP
wavy sediment sequences:
contouritic deposits ?
glacigenic debris
flows units
slide blocks
04JM059
length: 39.6 km
Time (ms)

The strongest point in our indirect dating of the slide is however the post-slide sediment infill on the southern escarpment and downslope from it (Fig. 4). As mentioned above, this sediment infill is up to 150 m thick, and therefore probably contains a significant glacial component. Furthermore, the seismic signature of the sediment body overlying the headscarp suggests it to be stacked glacigenic debris flow deposition, derived from the Hinlopen ice-stream during advanced glacial times (Fig. 4). As such, the massive Hinlopen Slide, or at least its last phase, is thought to be pre-Holocene, and possibly pre-dates the Last Glacial Maximum. This is in agreement with preliminary datings from planktonic foraminifera in a sediment core from the western rim of the slide complex [37].

From the morphological data, we know that the Hinlopen Slide complex consists of a multitude of slip planes and escarpments. Whether this morphology is the result of one single event in which the different phases happened within near succession in time or in several episodes well spread over time is not clear from our dataset.

4.3. Comparison with other major submarine slope failures

To fully understand the importance of the Hinlopen Slide, we compare its characteristics and especially its dimensions with other well-documented high-latitude slope failures on the Norwegian–Barents continental margin (e.g. Storegga, Trænadjupet, Andøya, Nyk, Bear Island slides) complemented with key examples from other geological and tectonic settings, e.g. from a prograding river-fed margin (Big'95 slide, continental slope of the Ebro margin in the north-western Mediterranean Sea) and from a volcanic ocean margin flank (Canary Slide on the north-western slope of El Hierro, Canary Island archipelago) (Fig. 6) [2–5,9,47–50].

From this compilation, it appears that most high-latitude slides including the Hinlopen Slide are translational in nature, and developed retrogressively in multiple phases [2]. This is, however, not confirmed for the Bear Island and Andøya slides. The high-latitude slope failures all lie proximal to high sediment delivery areas dominated by alternations between glacigenic debris flow and contouritic sediments, which is again not different for the Hinlopen Slide. Additionally, the slide scar areas and displaced volumes of high-latitude slides are typically much larger than slope failures occurring on the river-fed or volcanic margins.

Amongst the slope failures on glacially-influenced margins, the slide scar area of the Hinlopen Slide is not exceptional, and covers only c. 5% of the Storegga Slide scar area. Despite this modest slide scar area, the estimated volume released by the Hinlopen Slide is surprisingly high, involving roughly half of the mobilized volume in Storegga. This is remarkable, since drainage through the Hinlopen Trough is smaller compared to the drainage areas where large landslides have occurred off Norway, or other places along the northern margin of the Quaternary Eurasian ice sheet where major ice streams have fed the upper margin resulting in extensive trough mouth fan systems without leading to massive failure (e.g. the transverse trough between Nordaustlandet and Kvitøya (Fig. 1) or the Franz Victoria Trough further east [20]). This implies that large-scale mass wasting processes can occur in areas with less extensive sediment input.

One of the most extraordinary characteristics of the Hinlopen Slide is the maximum height of its escarpment surpassing 1400 m, which is four to five times higher compared to the maximum Storegga Slide escarpment, and even more compared to the other slides, except for the Canary Island slide. The latter has a reported headwall height of c. 1100 m [50], which is comparable to the escarpment height of the Hinlopen Slide. The dimensions of the rafted blocks are another peculiar feature of the Hinlopen Slide, both in footprint (5.4 by 2.1 km) and height (up to 450 m). Only the footprints of rafted blocks mobilized by the Big'95 slide appear larger (12.5 by 3.0 km), but these blocks rise only c. 20 m above the seabed. The rafted blocks involved in the Storegga Slide are approximately 30 times smaller in footprint (1.8 by 0.2 km) than those involved in the Hinlopen Slide, whereas the heights of the rafted blocks off Hinlopen are 6 to 7 times higher than those in the Storegga area.

As such, we conclude that the Hinlopen Slide is a unique feature and another giant submarine slope failure on the (formerly) glaciated Norwegian–Barents–Svalbard margin.

Fig. 5. (A) Seismic profile 04JM058 across the western sidewall of the Hinlopen Slide complex showing extensive, semi-transparent, chaotic sediment facies adjacent to the slide scar area. These sediments are interpreted as rapidly deposited stacked debris flow units related to ice stream dynamics through the Hinlopen Trough and pushed beyond the shelf break forming prograding fans. The sidewall measures c. 170 m, whereas minor escarpments are observed further to the west. Several large slide blocks are present within the slide scar. (B) Seismic profile 04JM059 across the eastern shoulder of the Hinlopen Slide complex reveals a different signature compared to its western counterpart. This profile illustrates the presence of similar semi-transparent glacigenic debris flow units as well as wavy sequences interpreted as contourites. The maps show the location of the seismic profiles.

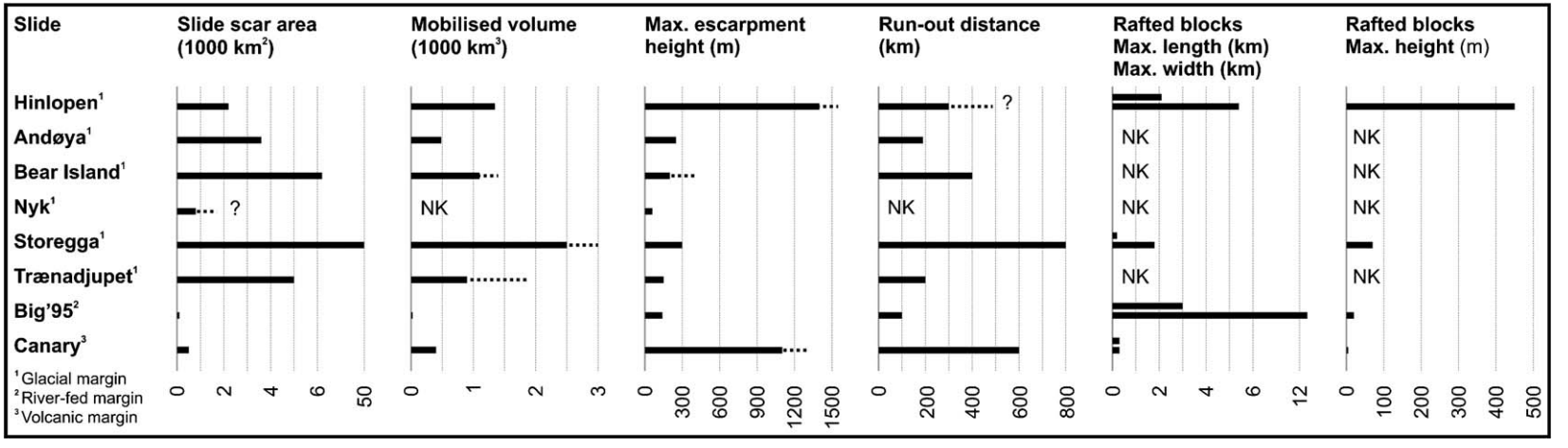

Fig. 6. Characteristics and dimensions of several submarine slope failures. All these slope failures except the Canary slide are translational and developed in multiple phases in a retrogressive way (not confirmed for Andøya and Bear Island slides). The Hinlopen Slide is exceptional in terms of released volume considering the relatively small slide scar area, the height and footprint of the rafted blocks, and the maximum escarpment height. For further discussion, see text. Data compiled from [2–5,9,47–50]. For location of the slides on the Norwegian margin, see Fig. 1. For the location of the Big'95 and Canary slides, see [2]. (NK = not known).

4.4. Could the Hinlopen Slide have generated a tsunami?

Based on the dimensions and setting of the Hinlopen Slide compared to other submarine slides known to have generated tsunamis, we can draw some preliminary conclusions about the potential of the slide to generate tsunamis. However, a number of specific uncertainties are involved in assessing the tsunami potential of the Hinlopen Slide. The most important ones are the *multi-phase, retrogressive nature of the slide* and the presently *unknown effect of the sea ice cover* at the time of failure.

Released volume, velocity and initial acceleration of the moving mass are key parameters to whether a tsunami will be initiated [12], but also the thickness of the dislodged masses plays a role [51]. Additionally, the actual wave structure and its amplitude will depend on the time lag between the individual failure phases in the supposedly retrogressive failure process, which may result in either constructive or destructive wave interference [35,51–53]. This time lag is presently unknown for the Hinlopen sliding phases. Numerical simulation has shown that slide volumes from 5 km^3, i.e. about 2.5 times the volume of the biggest rafted block, are capable of creating tsunami waves a few metres high [53], whereas the Storegga tsunami with amplitudes exceeding 20 m originated from the displacement of c. 2500 km^3 of sediments with a thickness of maximum 400 m [35,53]. Consequently, the displacement of 1350 km^3 of sediment with an average thickness of c. 610 m (maximum 1400 to 1500 m), or individual slabs of this large body, would normally generate a serious tsunami. Given the slightly steeper dip of the northern Svalbard margin and slip surfaces, a higher velocity and initial acceleration can be anticipated, which would increase the tsunami potential. This suggests that, in the worst-case scenario where constructive interference of the waves generated by the individual slabs occurs, the Hinlopen Slide could have resulted in a devastating tsunami affecting the Arctic Ocean and the Barents Sea.

There is one additional factor of uncertainty that needs to be incorporated in tsunami modelling in Polar Regions, i.e. the possible presence of sea ice at the time of failure. The northern Svalbard margin is even today nearly permanently covered by sea ice and it is reasonable to assume that the sea ice cover was larger and probably thicker during colder periods. This implies that it is unlikely for the slide to have happened during complete ice-free conditions. The role of sea ice covering the continental margin on tsunami amplitudes created by submarine slides in relatively deep waters is unknown. To our knowledge, no attempts have been undertaken yet to study and model tsunami hazards in such a particular setting, so one can only speculate on some scenarios that may happen. It could for instance be possible that the strength of the sea ice is strong enough to resist the movement in the water column, and as a result the ice may dampen the tsunami. Alternatively, the energy released by the mass movement and injected into the entire water column may exceed the strength of ice which could then break up. This could result in ice drifting and eventually affect ocean circulation processes. If so, the sedimentary record in the northern North-Atlantic and Arctic Oceans may show evidence of sea ice rafting episodes derived from such catastrophic events as well.

In the last 20 years, many past tsunamis have been recognised in geological settings from their specific deposits which have been left on tidal flats, marshes, lagoons and in coastal lakes [12]. So far, no one has searched for tsunami deposits along the lowlands surrounding the Arctic Ocean. In case a tsunami was generated, could it have inundated the coastal lowlands surrounding the Arctic Ocean? The extent of the glaciers onto the northern Svalbard shelf during the late Weichselian is debated, but glaciers could have reached the shelf break during glacial times [22,23]. In case the Hinlopen Slide occurred when glaciers extended beyond the coastline, the tsunami would have been prevented from reaching land. Tsunami deposits from this event would therefore probably only be discovered in case the landslide happened when glaciers had already retreated to the coastlines or further inland. Tsunami traces could furthermore have been removed by subsequent glaciation, in case the slide predates the LGM.

To sum up, the Hinlopen Slide had the capacity to generate a devastating tsunami based on the dimensions of the slide and the steep slope angle. Our dataset and results call for an increased focus on accurately dating the Hinlopen Slide phases, and to incorporate timing and slide displacement history as well as the effect of sea ice into advanced tsunami modelling, as it presents an important and interesting problem.

5. Conclusions

Swath bathymetry data reveal the complex slide scar geomorphology of a giant, submarine slope failure, the first mega-slide mapped in the Arctic Ocean. The slide has a multitude of steep escarpments (up to 35°) and gently dipping slip surfaces (<3°). From the morphology and its spatial variability, we infer that the Hinlopen Slide was a multi-phase, translational landslide that developed retrogressively.

The displaced volume, the escarpment heights and the dimensions of the rafted blocks give the Hinlopen

Slide its unique character, taking into account the relatively small slide scar and drainage areas. Although its slide scar area is only a fraction of Storegga's (c. 5%), the Hinlopen Slide nevertheless remobilized a volume of c. 1350 km^3, which is roughly half of that of the Storegga Slide. The maximum headwall height measures an unprecedented 1400 m, which could have contributed to the high mobility of the Hinlopen Slide. The largest rafted block is 452 m high, comprising a volume of 1.89 km^3. Both the escarpment heights and dimensions of the rafted blocks are an order of magnitude higher for the Hinlopen Slide than similar features in other well-studied submarine slope failures.

The location of the headwall in front of a prominent cross-shelf trough and the presence of both stacked glacigenic debris flow deposits as well as geotechnically-weaker contourites, suggest a climatic control on slope failure off northern Svalbard, similar to the Storegga Slide scenario. The timing of the Hinlopen Slide and development of its individual phases is not clear yet; however, the infill of the slide scar by glacigenic sediments derived from the Hinlopen Trough implies a pre-Holocene age, with triggering likely to be seismicity due to glacio-isostatic movement.

The setting and slide parameters also suggest that the Hinlopen Slide had the potential to create a devastating tsunami. Whether or not this was the case most likely depended on the multi-phase, retrogressive nature of the slide as well as on the effect of sea ice at the time of failure, and could have implications for the ice-rafted debris record in sediment cores from the Arctic Ocean. These parameters should be included in in-depth tsunami modelling due to submarine slope failures in Polar Regions.

Acknowledgements

All data presented in this paper were acquired during the R/V Jan Mayen (University of Tromsø) expedition in October 2004, in the framework of the European Science Foundation (ESF) project EUROMARGINS funded by the Norwegian Research Council (NFR Grant 158733/V30). We are very grateful to Steinar Iversen, Shaoli Yang, captain and crew for their efforts and support during data collection. Special thanks to Jan Sverre Laberg, Stein Bondevik, and other colleagues at the Department of Geology for fruitful discussions. Lindsay Wilson improved the English. Miquel Canals and Roger Urgeles provided the numbers for the slide scar areas for Big'95 and Canary slides. We also extend our gratitude to Anders Solheim, an anonymous reviewer and Editor Peggy Delaney for their constructive comments and feedback. Maps were created with Generic Mapping Tools (GMT). Roger Olaussen (Norwegian Polar Institute) provided the updated coastline for Kvitøya, whereas the Norwegian Petroleum Directorate (www.npd.no) provided the main structural elements shown in Fig. 1.

References

[1] J. Locat, J. Mienert (Eds.), Submarine Mass Movements and Their Consequences, Kluwer Academic Publishers, Dordrecht, 2003, 540 pp.
[2] M. Canals, G. Lastras, R. Urgeles, J.L. Casamor, J. Mienert, A. Cattaneo, M. De Batist, H. Haflidason, Y. Imbo, J.S. Laberg, Slope failure dynamics and impacts from seafloor and shallow sub-seafloor geophysical data: case studies from the COSTA project, Marine Geology 213 (2004) 9–72.
[3] H. Haflidason, H.P. Sejrup, A. Nygard, J. Mienert, P. Bryn, R. Lien, C.F. Forsberg, K. Berg, D. Masson, The Storegga Slide: architecture, geometry and slide development, Marine Geology 213 (2004) 201–234.
[4] J.S. Laberg, T.O. Vorren, The Trænadjupet Slide, offshore Norway — morphology, evacuation and triggering mechanisms, Marine Geology 171 (2000) 95–114.
[5] J.S. Laberg, T.O. Vorren, J.A. Dowdeswell, N.H. Kenyon, J. Taylor, The Andøya Slide and the Andøya Canyon, north-eastern Norwegian–Greenland Sea, Marine Geology 162 (2000) 259–275.
[6] A. Solheim, K. Berg, C.F. Forsberg, P. Bryn, The Storegga Slide complex: repetitive large scale sliding with similar cause and development, Marine and Petroleum Geology 22 (2005) 97–107.
[7] T.O. Vorren, Subaquatic landsystems: continental margins, in: D.J.A. Evans (Ed.), Glacial Landsystems, Arnold Publishers, London, 2003, pp. 289–312.
[8] N.-A. Mörner, Intense earthquakes and seismotectonics as a function of glacial isostasy, Tectonophysics 188 (1991) 407–410.
[9] M.A. Maslin, M. Owen, S. Day, D. Long, Linking continental-slope failures and climate change: testing the clathrate gun hypothesis, Geology 32 (2004) 53–56.
[10] P. Bryn, K. Berg, M.S. Stoker, H. Haflidason, A. Solheim, Contourites and their relevance for mass wasting along the mid-Norwegian Margin, Marine and Petroleum Geology 22 (2005) 85–96.
[11] K.Y. Vinnikov, A. Robock, R.J. Stouffer, J.E. Walsh, C.L. Parkinson, D.J. Cavalieri, J.F.B. Mitchell, D. Garrett, V.F. Zakharov, Global warming and northern hemisphere sea ice extent, Science 286 (1999) 1934–1937.
[12] S. Bondevik, J. Mangerud, S. Dawson, A. Dawson, O. Lohne, Evidence for three North Sea tsunamis at the Shetland Islands between 8000 and 1500 years ago, Quaternary Science Reviews 24 (2005) 1757–1775.
[13] D.R. Tappin, P. Watts, T. Matsumoto, Architecture and failure mechanism of the offshore slump responsible for the 1998 Papua New Guinea tsunami, in: J. Locat, J. Mienert (Eds.), Submarine Mass Movements and Their Consequences, Advances in Natural and Technological Hazards Research, vol. 19, Kluwer Academic Publishers, Dordrecht, 2003, pp. 383–389.
[14] D. Zwartz, P. Tregoning, K. Lambeck, P. Johnston, J. Stone, Estimates of present-day glacial rebound in the Lambert Glacier region, Antarctica, Geophysical Research Letters 26 (1999) 1461–1464.

[15] C. Kreemer, W.E. Holt, What caused the March 25, 1998 Antarctic plate earthquake?: inferences from regional stress and strain rate fields, Geophysical Research Letters 27 (2000) 2297–2300.
[16] K. Fleming, K. Lambeck, Constraints on the Greenland ice sheet since the last glacial maximum from sea-level observations and glacial-rebound models, Quaternary Science Reviews 23 (2004) 1053–1077.
[17] W. Krabill, E. Hanna, P. Huybrechts, W. Abdalati, J. Cappelen, B. Csatho, E. Frederick, S. Manizade, C. Martin, J. Sonntag, R. Swift, R. Thomas, J. Yungel, Greenland ice sheet: increased coastal thinning, Geophysical Research Letters 31 (2004) L24402, doi:10.1029/2004GL021533.
[18] O. Eiken, Seismic Atlas of Western Svalbard, Norsk Polarinstitutt, Oslo, 1994.
[19] W. Jokat, The sedimentary structure of the Lomonosov Ridge between 88°N and 80°N, Geophysical Journal International 163 (2005) 698–726.
[20] D. Ottesen, J.A. Dowdeswell, L. Rise, Submarine landforms and the reconstruction of fast-flowing ice streams within a large Quaternary ice sheet: the 2500-km-long Norwegian–Svalbard margin (57°–80°N), Geological Society of America Bulletin 117 (2005), doi:10.1130/B25577.25571.
[21] F.A. Butt, A. Elverhøi, A. Solheim, C.F. Forsberg, Deciphering late Cenozoic development of the western Svalbard margin from ODP site 986 results, Marine Geology 169 (2000) 373–390.
[22] K. Lambeck, Limits on the areal extent of the Barents Sea ice sheet in Late Weichselian time, Global and Planetary Change 12 (1996) 41–51.
[23] J.I. Svendsen, H. Alexanderson, V.I. Astakhov, I. Demidov, J.A. Dowdeswell, S. Funder, V. Gataullin, M. Henriksen, C. Hjort, M. Houmark-Nielsen, Late Quaternary ice sheet history of northern Eurasia, Quaternary Science Reviews 23 (2004) 1229–1271.
[24] W.H. Geissler, W. Jokat, A geophysical study of the northern Svalbard margin, Geophysical Journal International 158 (2004) 50–66.
[25] J.A. Dowdeswell, C.Ó Cofaigh, J. Taylor, N.H. Kenyon, J. Mienert, M. Wilken, On the architecture of high-latitude continental margins: the influence of ice-sheet and sea-ice processes in the Polar North Atlantic, in: J.A. Dowdeswell, C.Ó Cofaigh (Eds.), Glacier-Influenced Sedimentation on High-Latitude Continental Margins Special Publication, vol. 203, Geological Society, London, London, UK, 2002, pp. 33–54.
[26] N. Koc, D. Klitgaard-Kristensen, K. Hasle, C.F. Forsberg, A. Solheim, Late glacial palaeoceanography of Hinlopen Strait, northern Svalbard, Polar Research 21 (2002) 307–314.
[27] A.M. Myhre, J. Thiede, North-Atlantic–Arctic gateways, in: A.M. Myhre, J. Thiede, J.V. Firth (Eds.), Proceedings of the Ocean Drilling Program, Initial Reports 151, Ocean Drilling Program, College Station, 1995, pp. 5–26.
[28] M.A. Slubowska, N. Koc, T.L. Rasmussen, D. Klitgaard-Kristensen, Changes in the flow of Atlantic water into the Arctic Ocean since the last deglaciation: evidence from the northern Svalbard continental margin, 80°N, Paleoceanography 20 (2005) PA4014, doi:10.1029/2005PA001141.
[29] P. Wessel, W.H.F. Smith, Improved version of the generic mapping tools released, EOS Transactions of the American Geophysical Union 79 (1998) 579.
[30] N.Z. Cherkis, M.D. Max, P.R. Vogt, K. Crane, A. Midthassel, E. Sundvor, Large-scale mass wasting on the north Spitsbergen continental margin, Arctic Ocean, Geo-Marine Letters 19 (1999) 131–142.
[31] T. Bugge, S. Befring, R.H. Belderson, T. Eidvin, E. Jansen, N.H. Kenyon, H. Holtedahl, H.P. Sejrup, A giant three-stage submarine slide off Norway, Geo-Marine Letters 7 (1987) 191–198.
[32] J. Taylor, J.A. Dowdeswell, N.H. Kenyon, C.Ó. Cofaigh, Late Quaternary architecture of trough-mouth fans: debris flows and suspended sediments on the Norwegian margin, in: J.A. Dowdeswell, C.Ó Cofaigh (Eds.), Glacier-Influenced Sedimentation on High-Latitude Continental Margins Special Publication, vol. 203, Geological Society, London, London, UK, 2002, pp. 55–71.
[33] T.J. Kvalstad, L. Andresen, C.F. Forsberg, K. Berg, P. Bryn, M. Wangen, The Storegga Slide: evaluation of triggering sources and slide mechanics, Marine and Petroleum Geology 22 (2005) 245–256.
[34] T. Ilstad, F.V. DeBlasio, A. Elverhøi, C.B. Harbitz, L. Engvik, O. Longva, J.G. Marr, On the frontal dynamics and morphology of submarine debris flows, Marine Geology 213 (2004) 481–497.
[35] S. Bondevik, F. Løvholt, C. Harbitz, J. Mangerud, A. Dawson, J. Inge Svendsen, The Storegga Slide tsunami-comparing field observations with numerical simulations, Marine and Petroleum Geology 22 (2005) 195–208.
[36] P. Bryn, K. Berg, C.F. Forsberg, A. Solheim, T.J. Kvalstad, Explaining the Storegga Slide, Marine and Petroleum Geology 22 (2005) 11–19.
[37] D. Winkelmann, W. Jokat, F. Niessen, R. Stein, A. Winkler, Age and extent of the Yermak Slide north of Spitsbergen, Arctic Ocean, Geochemistry Geophysics Geosystems (submitted for publication).
[38] T. Mulder, P. Cochonat, Classification of offshore mass movements, Journal of Sedimentary Geology 66 (1996) 43–57.
[39] H.P. Kleiber, J. Knies, F. Niessen, The Late Weichselian glaciation of the Franz Victoria Trough, northern Barents Sea: ice sheet extent and timing, Marine Geology 168 (2000) 25–44.
[40] B.O. Hjelstuen, A. Elverhøi, J.I. Faleide, Cenozoic erosion and sediment yield in the drainage area of the Storfjorden Fan, Global and Planetary Change 12 (1996) 95–117.
[41] M. Hald, T. Dokken, G. Mikalsen, Abrupt climatic change during the last interglacial–glacial cycle in the Polar North Atlantic, Marine Geology 176 (2001) 121–137.
[42] M.A. Hampton, H.J. Lee, J. Locat, Submarine landslides, Reviews of Geophysics 34 (1996) 33–59.
[43] P. Gauer, T.J. Kvalstad, C.F. Forsberg, P. Bryn, K. Berg, The last phase of the Storegga Slide: simulation of retrogressive slide dynamics and comparison with slide-scar morphology, Marine and Petroleum Geology 22 (2005) 171–178.
[44] J.F. Dehls, O. Olesen, H. Bungum, E.C. Hicks, C.D. Lindholm, F. Riis, Neotectonic map: Norway and adjacent areas, Geological Survey of Norway (2000).
[45] D.J.W. Piper, P. Cochonat, M.L. Morrison, The sequence of events around the epicentre of the 1929 Grand Banks earthquake: initiation of debris flows and turbidity current inferred from sidescan sonar, Sedimentology 46 (1999) 79–97.
[46] D.C. Mosher, D.J.W. Piper, D.C. Campbell, K.A. Jenner, Near-surface geology and sediment-failure geohazards of the central Scotian Slope, American Association of Geologists, Bulletin 88 (2004) 703–723.
[47] B. Lindberg, J.S. Laberg, T.O. Vorren, The Nyk Slide—morphology, progression, and age of a partly buried submarine slide offshore northern Norway, Marine Geology 213 (2004) 277–289.
[48] J. Taylor, J.A. Dowdeswell, M.J. Siegert, Late Weichselian depositional processes, fluxes, and sediment volumes on the

margins of the Norwegian Sea (62–75°N), Marine Geology 188 (2002) 61–77.
[49] M. Canals, R. Urgeles, in: M. Vanneste (Ed.), Slide Scar Areas of Big'95 and Canary Island Slides, 2005.
[50] R. Urgeles, M. Canals, J. Baraza, B. Alonso, D.G. Masson, The most recent megalandslides of the Canary Islands: El Golfo debris avalanche and Canary debris flow, west El Hierro Island, Journal of Geophysical Research 102 (1997) 20,305–320,323.
[51] K.B. Haugen, F. Løvholt, C.B. Harbitz, Fundamental mechanisms for tsunami generation by submarine mass flows in idealised geometries, Marine and Petroleum Geology 22 (2005) 209–217.
[52] N.W. Driscoll, J.K. Weissel, J.A. Goff, Potential for large-scale submarine slope failure and tsunami generation along the U.S. mid-Atlantic coast, Geology 28 (2000) 407–410.
[53] F. Løvholt, C.B. Harbitz, K.B. Haugen, A parametric study of tsunamis generated by submarine slides in the Ormen Lange/ Storegga area off western Norway, Marine and Petroleum Geology 22 (2005) 219–231.